Chaos, Solitons and Fractals 131 (2020) 109501

Contents lists available at ScienceDirect

Chaos, Solitons and Fractals

Nonlinear Science, and Nonequilibrium and Complex Phenomena

journal homepage: www.elsevier.com/locate/chaos

Chaotic maps with nonlocal coupling: Lyapunov exponents, synchronization of chaos, and characterization of chimeras

Carlos A.S. Batista[a], Ricardo L. Viana[b,*]

[a] Centro de Estudos do Mar, Universidade Federal do Paraná, Curitiba, Paraná, Brazil
[b] Departamento de Física, Universidade Federal do Paraná, Curitiba, Paraná, Brazil

ARTICLE INFO

Article history:
Received 20 August 2019
Revised 9 October 2019
Accepted 25 October 2019
Available online 5 November 2019

Keywords:
Coupled map lattices
Nonlocal coupling
Chimeras
Lyapunov spectrum
Chaos synchronization

ABSTRACT

Coupled map lattices are spatially extended systems in which both space and time are discrete but allowing a continuous state variable. They have been intensively studied since they present a rich spatiotemporal dynamics, including intermittency, chimeras, and turbulence. Nonlocally coupled lattices occur in many problems of physical and biological interest, like the interaction among cells mediated by the diffusion of some chemical. In this work we investigate general features of the nonlocal coupling among maps in a regular lattice, focusing on the Lyapunov spectrum of coupled chaotic maps. This knowledge is useful for determining the stability of completely synchronized states. One of the types of nonlocal coupling investigated in this work is a smoothed finite range coupling, for which chimeras are exhibited and characterized using quantitative measures.

1. Introduction

Coupled map lattices have been used for a long time as mathematical models of spatially extended dynamical systems, for which both space and time are discrete, but allowing a continuous state variable [1]. One way to derive such spatially extended systems is to consider a diffusion-reaction system (partial differential equation) with a pulsed reaction term [2], what provides a natural way to discretize the time evolution. In this case coupling is generated by discretizing the second spatial derivative contained in the diffusion term, resulting in a lattice where each site is coupled to its nearest neighbors. Such locally coupled lattices were studied by Kaneko since the early 1980's, with a wealth of numerical results available [3,4].

One of the outstanding dynamical phenomena presented by such system is the capability of synchronize complicated motions due to the coupling effect. The phenomenon of collective synchronization of flashing fireflies has brought into attention another form of coupling, in which each oscillator is coupled to the mean field produced by all other sites [5]. This kind of global coupling was popularized by the Kuramoto model of coupled oscillator [6], and adapted to coupled map lattices by Kaneko, who investigated many properties of this type of nonlocal coupling [7,8].

The general characteristic of nonlocal couplings is the interaction among a given site with all its neighbors. Kuramoto has provided an interesting physical setting where such coupling arise naturally: an assembly of oscillator ("cells") is such that their coupling is mediated by the diffusion of some chemical [9]. This chemical is released by each oscillator with a rate dependent of its own dynamics, and the latter is affected by the local concentration of that chemical [10]. If the diffusion time is so short that the chemical concentration relaxes immediately to its equilibrium value, it has been shown that the coupling intensity decays exponentially with the lattice distance, in the one-dimensional case [11]. The dynamical properties of such lattices have been recently investigated, such as bursting synchronization [12], frequency synchronization [13] and complete synchronization of chaos [14].

One of the outstanding biological problems which can be modeled using a type of nonlocal coupling, where the coupling strength depends in some way on the individual dynamics of the cells is the synchronization among cells of the suprachiasmatic nucleus (SCN) in the brain hypothalamus [15,16]. The SCN is an assembly of clock cells whose synchronized dynamics is responsible for the circadian rhythm in mammals [17,18]. The coupling among SCN cells is thought to be mediated by the release and absorption of a neurotransmitter like GABA or VIP [19–23].

A related kind of nonlocal coupling consists in considering the coupling strength as decreasing with the lattice distance as a power-law, instead of an exponential function [24]. Another form of nonlocal coupling consists on taking only a finite number of neighbors of a given site (finite range), and has been often used to

* Corresponding author.
E-mail address: viana@fisica.ufpr.br (R.L. Viana).

https://doi.org/10.1016/j.chaos.2019.109501
0960-0779/

investigate complicated spatiotemporal patterns like chimeras [25–27]. Trigonometric forms for the nonlocal dependence have been given much attention [28–30]. A current line of investigation involves the design of coupling functions capable of yielding desired responses, like synchronization and oscillator death [31,32].

In this work we propose a general approach to coupled map lattices with nonlocal coupling represented by a range function which has a small number of mathematical requirements. The known expressions for coupling show up as particular choices of the range function. We explore some dynamical properties of such coupled lattices, like the Lyapunov spectrum for a lattice of coupled piecewise linear chaotic maps, where analytical results can be obtained [33,34]. This knowledge is useful to determine the transversal stability properties of the completely synchronized state [35]. Examples are given for a smoothed finite range coupling, which can be used to investigate differences among smooth and piecewise linear range functions. Moreover, we consider also the formation of chimera in lattices of coupled chaotic maps with smoothed finite range coupling, and applied some numerical diagnostics of spatial coherence. One of these diagnostics is a local version of the well-known Kuramoto order parameter [25,26], which is able to distinguish spatially coherent from incoherent patterns. We count the plateaus of the local order parameter according to a measure of local coherence (average plateau size) [36].

This paper is organized as follows. Section 2 presents a general framework to describe long-range coupling, by introducing a range function. The Lyapunov spectrum of a coupled map lattice with a general range function is obtained in Section 3 for the case of coupled piecewise-linear chaotic maps. Section 4 contains an application of the Lyapunov spectrum to the transversal stability properties of a lattice of coupled chaotic maps. Numerical results on chimera formation and characterization for a smoothed finite-range coupling are shown in Section 5. The last Section contains our conclusions.

2. General long-range coupling

Most investigations of the spatiotemporal dynamics in discrete time use the so-called local coupling, in which each map $x \to f(x)$ is coupled to its nearest neighbors, in the form

$$x_{n+1}^{(i)} = (1-\varepsilon) f\left(x_n^{(i)}\right) + \frac{\varepsilon}{2}\left[f\left(x_n^{(i-1)}\right) + f\left(x_n^{(i+1)}\right)\right], \tag{1}$$

where $x_n^{(i)}$ is the state variable at discrete time n and belonging to a chain of N identical systems, such that $i = 1, 2, \ldots, N$; ε standing for the coupling strength. This type of coupling is also called laplacian since it represents the discretization of a second derivative with respect to the position along a one-dimensional lattice [3]. It is straightforwardly generalized to a higher-dimensional lattice.

By way of contrast, in a globally coupled map lattice, each map is coupled to the "mean field" generated by all other sites, irrespective of their relative position [7]

$$x_{n+1}^{(i)} = (1-\varepsilon) f\left(x_n^{(i)}\right) + \frac{\varepsilon}{N-1} \sum_{j=1, j\neq i}^{N} f\left(x_n^{(j)}\right), \tag{2}$$

In the following we will consider periodic boundary conditions: $x_n^{(i\pm N)} = x_n^{(i)}$ and appropriate initial conditions $x_0^{(i)}$, for $i = 1, \ldots N$.

This type of coupling is nonlocal, in the sense that it considers the coupling with other neighbors than the nearest ones. Many different nonlocal couplings have been proposed since then. The finite-range coupling is an immediate generalization of the local coupling, but it takes into account the P nearest neighbors of a given site in a lattice of N sites [dashed line in Fig. 1(a)] [25]:

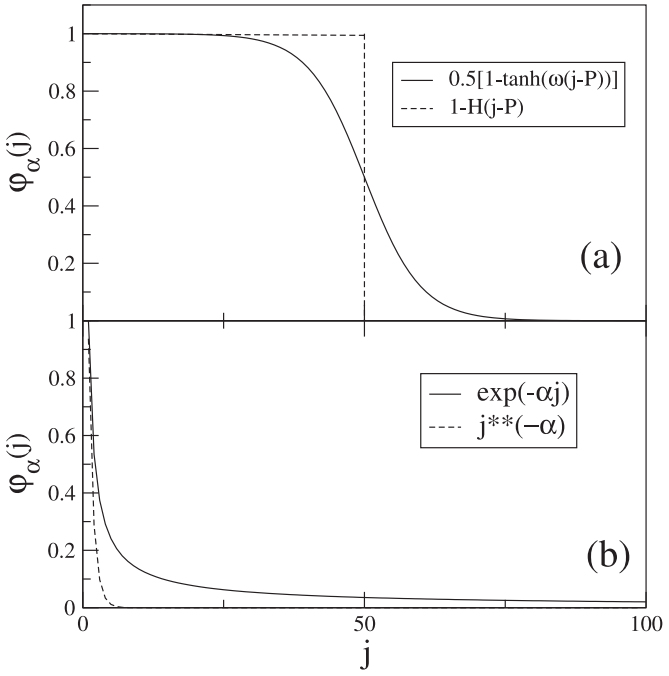

Fig. 1. Range function for some kinds of nonlocal coupling prescription: (a) finite range coupling (dashed line), smoothed finite-range coupling (full line); (b) exponential decay (full line), power-law decay (dashed line).

$$x_{n+1}^{(i)} = (1-\varepsilon) f\left(x_n^{(i)}\right) + \frac{\varepsilon}{2P} \sum_{j=1}^{P}\left[f\left(x_n^{(i-j)}\right) + f\left(x_n^{(i+j)}\right)\right], \tag{3}$$

where $P \leq N' = (N-1)/2$ is the coupling radius, which can vary between $P = 1$ (local coupling) to $P = (N-1)/2$ (global coupling). Similarly we can define a normalized coupling radius $r = P/N$. This coupling has been extensively used in numerical investigations of chimeras for coupled chaotic maps [26,27].

Another type of nonlocal coupling arises in models of pointlike dynamical systems (hereafter represented by maps) whose interaction is mediated by the fast diffusion of some chemical into the medium in which the systems are embedded [9]. In this case each system (like a biological cell) releases a chemical with a rate depending on its own dynamics. The dynamics of other maps is affected by the local concentration of this chemical. Kuramoto has shown that, provided the diffusion is fast enough, the coupling in one spatial dimension is nonlocal, the relative coupling strength decreasing exponentially with the lattice position with a decay rate α [full line in Fig. 1(b)] [10,11]:

$$x_{n+1}^{(i)} = (1-\varepsilon) f\left(x_n^{(i)}\right) + \frac{\varepsilon}{\eta(\alpha)} \sum_{j=1}^{N'} e^{-\alpha j}\left[f\left(x_n^{(i-j)}\right) + f\left(x_n^{(i+j)}\right)\right], \tag{4}$$

where $N' = (N-1)/2$ and the normalization factor is $\eta(\alpha) = 2\sum_{j=1}^{N'} e^{-\alpha j}$. It is easy to show that, if $\alpha \to 0$ we obtain the globally coupled lattice (2), whereas $\alpha \to \infty$ gives the local coupling (1). Hence we may consider α a variable range parameter.

A related model considers the relative coupling strength as decreasing with the lattice position in a power-law fashion with exponent α [dashed line in Fig. 1(a)] [24]:

$$x_{n+1}^{(i)} = (1-\varepsilon) f\left(x_n^{(i)}\right) + \frac{\varepsilon}{\eta(\alpha)} \sum_{j=1}^{N'} j^{-\alpha}\left[f\left(x_n^{(i-j)}\right) + f\left(x_n^{(i+j)}\right)\right], \tag{5}$$

where the normalization factor is $\eta(\alpha) = 2\sum_{j=1}^{N'} j^{-\alpha}$. The limiting behavior as α varies from zero to infinity is the same as be-

fore. This model has been used in various studies on the influence of coupling nonlocality in dynamical properties like synchronization [37–39], bubbling bifurcation [35], decay of spatial correlations [40], short-time memories [41], and collective behavior in neuronal networks [42].

These models can be treated as particular cases of a general long-range coupling given by

$$x_{n+1}^{(i)} = (1-\varepsilon) f\left(x_n^{(i)}\right) + \frac{\varepsilon}{\eta(\alpha)} \sum_{j=1}^{N'} \phi_\alpha(j) \left[f\left(x_n^{(i-j)}\right) + f\left(x_n^{(i+j)}\right) \right], \tag{6}$$

where the range function $\phi_\alpha(j)$ is a monotonically decreasing function of the lattice distance j. In the cases of our immediate interest, we have a monotonically decreasing function of j, such that $\phi_\alpha(s) \to 0$ for large j. However, this is not a mathematical requirement, and some range functions that have been used in the literature do not satisfy it, as trigonometric functions like $\phi_\alpha(j) = [1 + \alpha \cos(\pi j)]/2$ for example [28–30].

Apart from those cases, for the chemical coupling (4) we have a range function $\phi_\alpha(j) = \exp(-\alpha j)$, whereas for the power-law coupling (5) $\phi_\alpha(j) = j^{-\alpha}$, both monotonically decreasing with j. The finite range coupling (3) is such that $\alpha = 1 + [(2P+1)/N]$ and the range function is $\phi_\alpha(j) = 1 - H(j-P)$, where $H(x)$ is the Heaviside unit step function. In all those cases the normalization factor reads

$$\eta(\alpha) = 2 \sum_{j=1}^{N'} \phi_\alpha(j). \tag{7}$$

Note that, as $\alpha \to 0$ we have $\eta(\alpha) \to N-1$ and thus $\lim_{\alpha\to 0} \phi_\alpha(j) = 1$. On the other hand, if $\alpha \to \infty$ we have $\eta(\alpha) \to 2$ and thus $\lim_{\alpha\to\infty}(j) = \delta_{j1}$, which vanishes provided $j \neq 1$. Since the finite-range coupling is characterized by a piecewise continuous range function, it is interesting also to investigate the case of a smoothed finite range [full line in Fig. 1(b)]:

$$\phi_\alpha(j) = \frac{1}{2}\{1 - \tanh[\omega(j-P)]\}, \tag{8}$$

where ω is a smoothing parameter and the range parameter $\alpha = 1 + [(2P+1)/N]$ like in the finite-range coupling.

3. Lyapunov spectrum

The general coupling in Eq. (6) can be written in a compact way as

$$\mathbf{x}_{n+1} = \mathbf{F}(\mathbf{x}_n), \tag{9}$$

where $\mathbf{x}_n = (x_n^{(1)}, \ldots x_n^{(N)})^T$ and $\mathbf{F}$ is the corresponding vector field. We consider the tangent vector $\boldsymbol{\xi}_n = (\delta x_n^{(1)}, \ldots \delta x_n^{(N)})^T$, whose time evolution is given by linearizing the vector field of the coupled map lattice:

$$\boldsymbol{\xi}_{n+1} = \mathbf{T}_n \boldsymbol{\xi}_n, \tag{10}$$

where $\mathbf{T}_n = \mathbf{DF}(\mathbf{x}_n)$ is the Jacobian matrix.

We form the time-ordered product $\boldsymbol{\tau}_n = \mathbf{T}_{n-1} \ldots \mathbf{T}_1 \mathbf{T}_0$ and the corresponding matrix

$$\hat{\boldsymbol{\Lambda}} = \lim_{n\to\infty} \left(\boldsymbol{\tau}_n^T \boldsymbol{\tau}_n\right)^{1/2n}, \tag{11}$$

with eigenvalues $\{\Lambda_i\}_{i=1}^N$. The Lyapunov exponents are thus

$$\lambda_k = \ln \Lambda_k, \qquad (k = 1, 2, \ldots, N). \tag{12}$$

Changing the summation indices in (6) it is straightforward to show that the Jacobian matrix elements are

$$T_n^{(ik)} = (1-\varepsilon) f'\left(x_n^{(i)}\right)\delta_{ik} + \frac{\varepsilon}{\eta(\alpha)} \phi_\alpha(r_{ij}) f'\left(x_n^{(k)}\right)\left(1-\delta_{jk}\right), \tag{13}$$

where the primes denote differentiation with respect to the argument.

Let us consider as an example the Bernoulli map, for which $x \in [0, 1)$ and the map is piecewise linear, $f(x) = ax \pmod 1$, with constant slope $f'(x) = a$. If $a > 1$ the dynamics is strongly chaotic for almost all initial conditions (i.e., up to a measure zero set of eventually periodic points), with Lyapunov exponent $\ln a > 0$. Since we are working with periodic boundary conditions the corresponding Jacobian is a circulant matrix, whose eigenvalues are given by trigonometric sums, such that the Lyapunov exponents are given by

$$\lambda_k = \ln a + \ln\left|1 - \varepsilon\left(1 - \frac{b_k}{\eta(\alpha)}\right)\right|, \qquad (k = 1, 2, \ldots, N), \tag{14}$$

where

$$b_k = 2 \sum_{j=1}^{N'} \phi_\alpha(j) \cos\left(\frac{2\pi jk}{N}\right). \tag{15}$$

It is possible to obtain exact analytical expressions for the latter coefficients in the nonlocal types of coupling mentioned in the previous Section. In the cases of power-law and exponentially-decaying couplings the corresponding Lyapunov exponents were obtained in Refs. [33,34] and [14], respectively. For the finite-range coupling (3), for example, we have

$$b_k = 2 \sum_{j=1}^{P} \cos\left(\frac{2\pi jk}{N}\right) = -1 + \frac{\sin\left[\left(P + \frac{1}{2}\right)\frac{2\pi k}{N}\right]}{\sin\left(\frac{\pi k}{N}\right)} \tag{16}$$

where we used Lagrange's trigonometric identity. The Lyapunov spectrum is obtained plugging (16) into (14) and using $\eta(\alpha) = 2P$.

Let us examine the limiting cases of the resulting expression. For a global coupling $2P = N-1$ and we obtain immediately the well-known expression

$$\lambda_k = \begin{cases} \ln a + \ln\left|1 - \varepsilon \frac{N}{N-1}\right| & \text{for } k \neq N \\ \ln a, & \text{for } k = N \end{cases} \tag{17}$$

On the other hand, for local coupling we set $P = 1$ and obtain, after some elementary algebra,

$$\lambda_k = \ln a + \ln\left|1 - 2\varepsilon \sin^2\left(\frac{\pi k}{N}\right)\right| \tag{18}$$

Finally let us explore the case of a smoothed finite-range coupling, for which the range function is given by (8), with two variable parameters: the smoothness parameter ω and the normalized coupling radius $r = P/N$. For $\omega = 0$ we recover the abovementioned finite range coupling. The Lyapunov spectrum of a coupled map lattice built upon this prescription is shown in Fig. 2 for some values of ω and r. The spectrum is symmetric with respect to $k = N/2$. Most exponents take on values near 0.537. According to (17) the Lyapunov spectrum for a global coupling, which corresponds to a finite range coupling with maximum coupling radius $r = 0.5$, exhibits a $(N-1)$-fold degeneracy. This degeneracy is partially lifted for smaller coupling radius and is further modified by smoothing effects, as illustrated in Fig. 2(a): the Lyapunov exponents present "damped oscillations" around a constant value reminiscent of the degeneracy of the global case. In fact, for higher ω this effect is more pronounced, and the "damping" lasts longer (Fig. 2(b)).

4. Complete synchronization

Another instance where the knowledge of a closed-form expression for the Lyapunov exponent is useful is the analysis of the transversal stability of a completely synchronized state. For a coupled map lattice of the general form (6) with some map $f(x)$ it turns out that the completely synchronized state

$$x_n^{(1)} = x_n^{(2)} = \ldots x_n^{(N)} \equiv x_n^* \tag{19}$$

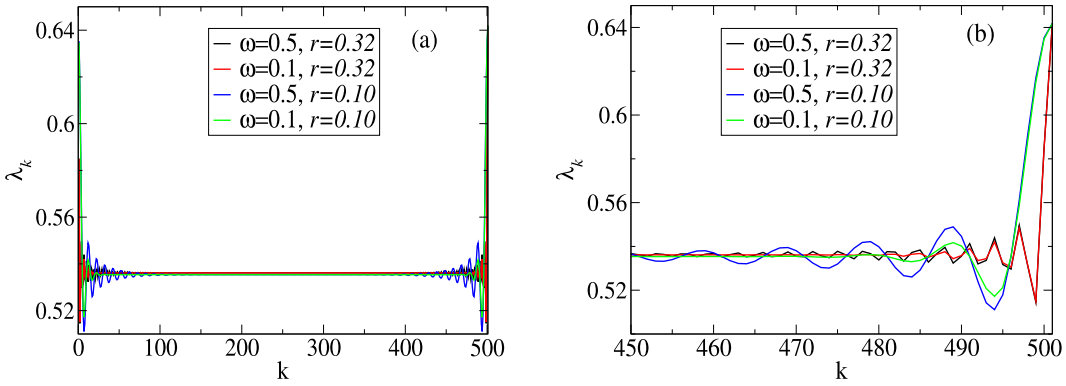

Fig. 2. (a) Lyapunov spectrum of the smoothed finite range coupling, (b) magnification of a selected region of (a).

is actually a solution since it implies that $x_n^* = f(x_n^*)$ for all times. A major question is, in this case, if this synchronization state is stable under general transversal perturbations.

Answering this question is equivalent to determine the eigenvalues of the matrix $\hat{\mathbf{\Lambda}}(x^*)$ computed in the completely synchronized state (19). One of the Lyapunov exponents is obviously along the synchronization manifold defined by (19). A similar calculation gives, for the $N-1$ remaining transversal Lyapunov exponents,

$$\lambda_k^* = \lambda_U + \ln\left|1 - \varepsilon\left(1 - \frac{b_k}{\eta(\alpha)}\right)\right|, \qquad (k = 1, 2, \ldots, N-1), \quad (20)$$

where λ_U is the Lyapunov exponent of each map. For example, the Ulam map $f(x) = 4x(1-x)$, with $x \in [0, 1)$, is topologically conjugate to the Bernoulli map with $a = 2$ and thus has $\lambda_U = \ln 2$, and so is strongly chaotic (transitive).

For the completely synchronized state to be transversely unstable it is sufficient to show that the maximal exponent is positive, i.e. $\lambda_2^* > 0$. It turns out that the synchronized state is transversely stable provided $\varepsilon_c \le \varepsilon \le \varepsilon'_c$, where

$$\varepsilon_c = \left(1 - e^{-\lambda_U}\right)\left(1 - \frac{b_1}{\eta(\alpha)}\right)^{-1}, \quad (21)$$

$$\varepsilon'_c = \left(1 - e^{-\lambda_U}\right)\left(1 - \frac{b_{N'}}{\eta(\alpha)}\right)^{-1}, \quad (22)$$

and, following (15),

$$b_1 = 2\sum_{j=1}^{N'} \phi_\alpha(j) \cos\left(\frac{2\pi j}{N}\right), \quad (23)$$

$$b_{N'} = 2\sum_{j=1}^{N'} \phi_\alpha(j) \cos\left(\frac{\pi(N-1)j}{N}\right), \quad (24)$$

This condition leads to accurate predictions of the loss of transversal stability of the completely synchronized state.

The loss of transversal stability of the completely synchronized state can also be numerically determined by computing the order parameter of the coupled map lattice (6), defined as [43,44]

$$z_n = R_n e^{i\varphi_n} = \frac{1}{N}\sum_{j=1}^{N} e^{2\pi i x_n^{(j)}}. \quad (25)$$

The quantities R_n and $\varphi_n \in [0, 2\pi)$ are respectively the amplitude and angle of a rotating vector equal to the vector sum of phasors for each state variable in a one-dimensional lattice with periodic boundary conditions. For a completely synchronized state the order parameter magnitude is $R_n = 1$ for all time n. On the other hand, in a completely non-synchronized state, for which the phase angles are uniformly distributed over $[0, 2\pi)$, $R_n \approx 0$. The case

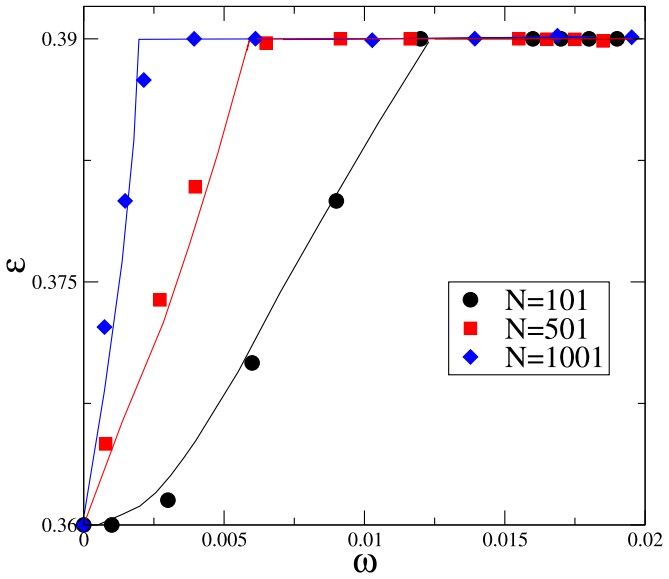

Fig. 3. Parameter values for which the completely synchronized state of the coupled map lattice (6) loses transversal stability, for different lattice sizes. The full lines represent the theoretical prediction based on the Lyapunov spectrum, whereas points represent numerical estimates based on the order parameter (25).

$0 < R_n < 1$ represents a partially synchronized state. We can numerically verify that the totally synchronized state has lost transversal stability if R_n (for a given time n so large that the transients have died out) becomes less than a specified threshold, namely 0.97 (small variations in this value do not produce substantial changes in our results).

In Fig. 3 we plot, in the parameter plane ε *versus* ω, the points for which the completely synchronized state has lost transversal stability, for different lattice sizes N. The full lines represent the theoretical values predicted by Eqs. (21)–(22), showing a good agreement with numerical values.

5. Chimeras for a smoothed finite-range coupling

A great deal of the current research involving chimeras is focused on non-locally coupled dynamical systems, from partial differential equations (like complex Ginzburg-Landau equation), to ordinary differential equations (like Rössler equations) and coupled map lattices. However, it should be remarked that the nonlocality of the coupling is not an essential condition for the existence of chimeras [45].

As for the latter, one of the most used non-local coupling prescriptions is the finite range (3). One outstanding feature of the

results obtained for this system is that there are chimeras which last during a large timespan. Up to some maximum value used in numerical simulations, one can say that those chimeras are permanent.

Other nonlocal coupling prescriptions, like power-law and chemical ones, however, typically show transient chimeras with quite small timespan. A fundamental difference between these forms and the finite range coupling is that the latter is piecewise continuous, whereas the former are smoothly decaying range functions. Hence the question arises whether or not the timespan of the chimeras could be related to the smoothness of the range function.

In the following we shall consider a nonlocally coupled lattice as given by (6), with the smoothed finite range coupling given by (8). The latter has a smoothing parameter γ which can be varied so as to investigate the transition between a piecewise continuous and a smooth nonlocal coupling prescription. The local dynamics is given by the logistic map $f(x) = ax(1-x)$, with $a = 3.8$, such that the uncoupled maps display chaotic behavior.

The numerical simulations we present in this Section were performed with a lattice of N sites, periodic boundary conditions: $x_n^{(i\pm N)} = x_n^{(i)}$ and initial condition profiles $x_0^{(i)}$ representing interpolations of periodic functions. Fig. 4 shows snapshots of the spatial pattern for $N = 501$ maps with coupling radius $r = 0.32$, which corresponds to $P = rN = 160$ neighbors at each side of a given map, and to a range parameter of $\alpha = 1 + [(2P+1)/N] = 1.64$. The smoothness parameter ω is kept fixed at 0.006, and varying coupling strength ε. Periodic initial conditions profile were used throughout.

For $\varepsilon = 0.39$ (Fig. 4(a)) a snapshot of the spatial pattern reveals a unique coherent pattern, which breaks down as ε is decreased (Fig. 4(c)) and results in a chimera with further decrease (Fig. 4(e)). This chimera eventually disappears into a completely incoherent state as we switch off the coupling (Fig. 4(g)).

We can describe the transition from a completely ordered to a completely disordered pattern by using the local order parameter proposed in Refs. [25,26]. Denoting by $\max_j\{x^{(j)}\}$ and $\min_j\{x^{(j)}\}$ the maximum and minimum values of x in a snapshot spatial pattern, respectively, we can define a geometrical phase for the jth map as [26]

$$\sin\psi_j = \frac{2x^{(j)} - \max_j\{x^{(j)}\} - \min_j\{x^{(j)}\}}{\max_j\{x^{(j)}\} - \min_j\{x^{(j)}\}}, \qquad (j = 1, 2, \ldots, N) \tag{26}$$

in such a way that a spatial half-cycle is mapped onto the phase interval $[-\pi/2, \pi/2]$. Note that this phase definition is slightly different from that used in Eq. (25), where we were interested on the loss of transversal stability of the completely synchronized state. Here we have to adapt this definition so as to deal with spatially coherent states, which do not need to be synchronized states.

The corresponding local order parameter magnitude is

$$R_k = \lim_{N\to\infty} \frac{1}{2\delta(N)} \left| \sum_{j\in C} e^{i\psi_j} \right|, \qquad (k = 1, 2, \ldots, N) \tag{27}$$

where the summation is restricted to the interval of j-values such that

$$C : \left| \frac{j}{N} - \frac{i}{N} \right| \le \delta(N), \tag{28}$$

where $\delta(N) \to 0$ for $N \to \infty$.

Basically the local order parameter quantifies the spatial order in the neighborhood of a given site, for it takes on values near the unity within coherent domains, and lesser values within incoherent domains in a chimera. In fact, the local order parameter is uniformly equal to the unity for the coherent pattern (Fig. 4(b)). Parts

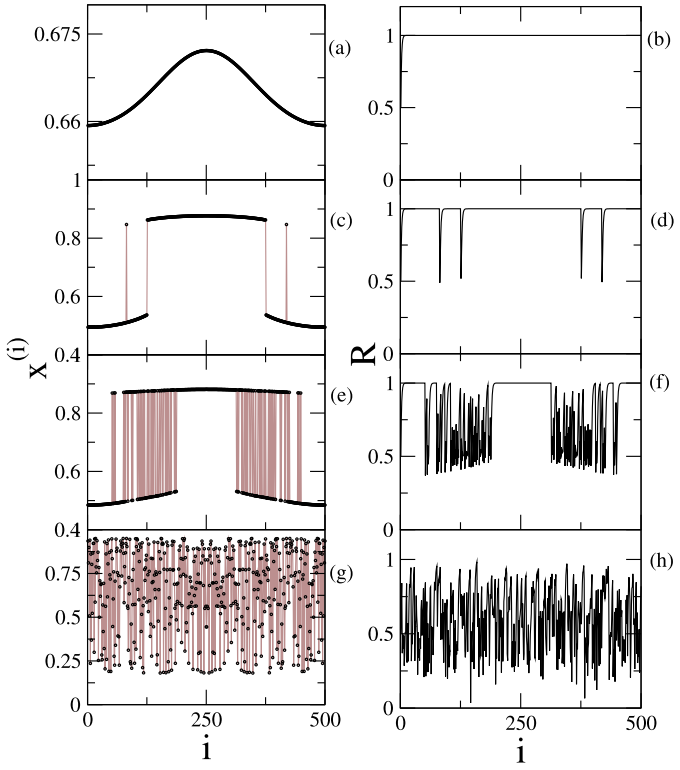

Fig. 4. Snapshots of the spatial pattern for $N = 501$ coupled chaotic logistic maps ($a = 0.38$) in the form (8), with normalized coupling radius $r = 0.32$ ($P = 160$), smoothness parameter $\omega = 0.006$ and coupling strength $\varepsilon =$ (a) 0.39; (c) 0.33, (e) 0.29, and (g) 0.0. (b), (d), (f) and (g) show the local order parameter corresponding to the snapshots at the lefthandside.

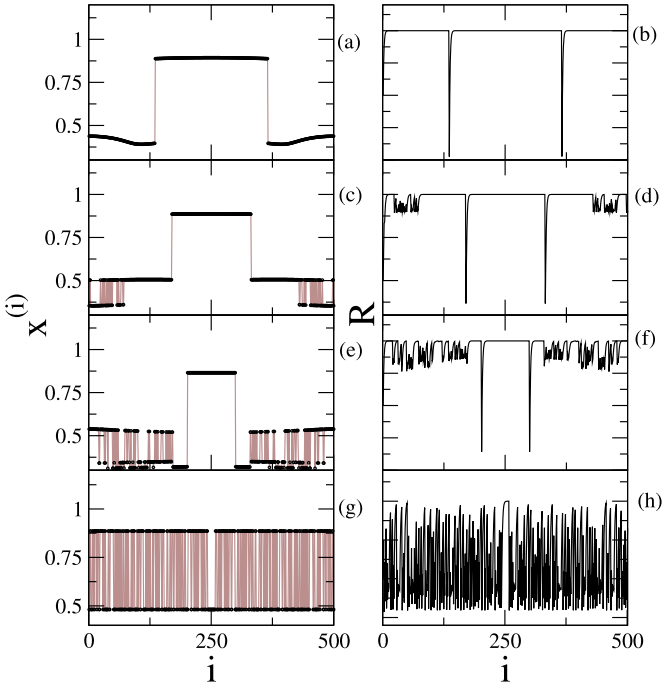

Fig. 5. Snapshots of the spatial pattern for $N = 501$ coupled chaotic logistic maps ($a = 0.38$) in the form (8), with normalized coupling radius $r = 0.32$ ($P = 160$), coupling strength $\varepsilon = 0.19$ and smoothness parameter ω and (a) 0.0020; (c) 0.0014, (e) 0.011, and (g) 0.0. (b), (d), (f) and (g) show the local order parameter corresponding to the snapshots at the lefthandside.

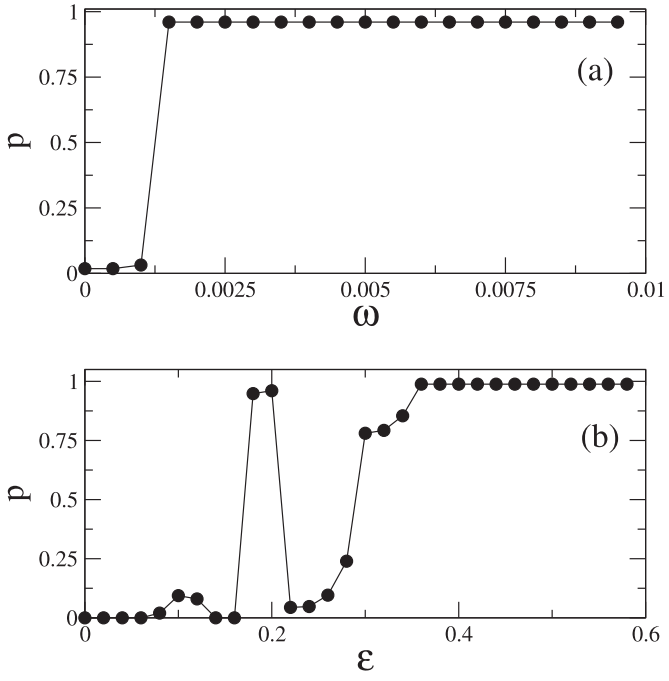

Fig. 6. (a) Degree of coherence as a function of ω for fixed $\varepsilon = 0.19$; (b) as a function of the coupling strength ε for a smoothness parameter $\omega = 0.006$. In both cases we considered a smoothed finite range coupling with normalized coupling radius $r = 0.32$ ($P = 160$).

of the spatial pattern outside coherent regions are marked by values of R_i between 0.0 and 1.0 (Fig. 4(d), (f) and (h)).

A similar analysis can be performed fixing the coupling strength (at $\varepsilon = 0.19$) and varying the smoothness parameter ω in order to investigate its effect on the nature of the chimeras. The sequence of spatial pattern snapshots is shown in Fig. 5 starting from $\omega = 0.0020$, for which there is practically no chimera (Figs. 5(a)-(b)) to a state of a nascent chimera (Fig. 5(c)-(d)) to a larger chimera (Fig. 5 (e)-(f)) and finally no chimera at all when the coupling is pure finite range (no smoothing) (Fig. 5(g)-(h)). We conclude that it is possible to generate chimeras by smoothing the finite range coupling.

With help of the local order parameter, and the fact that coherent regions in the snapshot patterns correspond to plateaus of $R_i = 1.0$, we can quantify the coherent content in a given chimera pattern by defining a quantity (degree of coherence) p by the relative mean plateau size [37]. Let N_i be the length of the ith coherence plateau, and N_p the total number of such plateaus. The mean plateau size is $\tilde{N} = (1/N_p)\sum_{i=1}^{N_p} N_i$, such that the coherence degree is $p = \tilde{N}/N$. If the snapshot exhibits a single coherent region [e.g., in Fig. 4(a)] there is just one plateau and $\tilde{N} = N$, hence $p = 1$. On the other hand, if the snapshot pattern is completely incoherent [e.g., as in Fig. 5(h)], we have $N_p \approx N$, $\tilde{N} \approx 1$ and $p \approx 1/N \to 0$ as $N \to \infty$.

The degree of coherence is plotted in Fig. 6(a) as a function of the coupling strength for a finite range coupling with smoothness parameter $\omega = 0.006$, and in Fig. 6(b) as a function of ω for fixed $\varepsilon = 0.19$. In both cases we have observed a transition from total incoherent to coherent behavior, as illustrated in Figs. 4 and 5. The sharpest transition here is obtained by varying ω, exhibiting a critical $\omega_c \approx 0.001$ (which turns out to be dependent of ε) (Fig. 6(b)). Fig. 6(a) also shows such a transition, for varying ε, but the transition is interrupted and resumed for $\varepsilon \lesssim 0.25$.

Actually both diagrams are cross-sections of the more complete phase diagram depicted in Fig. 7, which shows the degree of coherence (in color scale) *versus* both parameters, ε and ω. It is apparent that the changes in the smoothness parameter ω are more conspicuous when the coupling strength is either not very small or not very large, corresponding to a strip $0.2 \lesssim \varepsilon \lesssim 0.35$. Within this range the smoothing effect is complicated and depends on details of the spatio-temporal dynamics of the coupled map lattice.

We finish this Section by presenting results for different values of the normalized coupling radius, what brings about the possibility of multiple chimeras at non-symmetric positions along the lattice. In Fig. 8 we show snapshots of spatial patterns for coupling strength $\varepsilon = 0.29$ and smoothness parameter $\omega = 0.006$, with three different values of the coupling radius. The variation of the degree of coherence with ω and ε are depicted in Fig. 9(a) and (b), respectively, for two values of the coupling radius. These results suggest that the present diagnostic of spatial coherence is useful in situations with multiple chimera states.

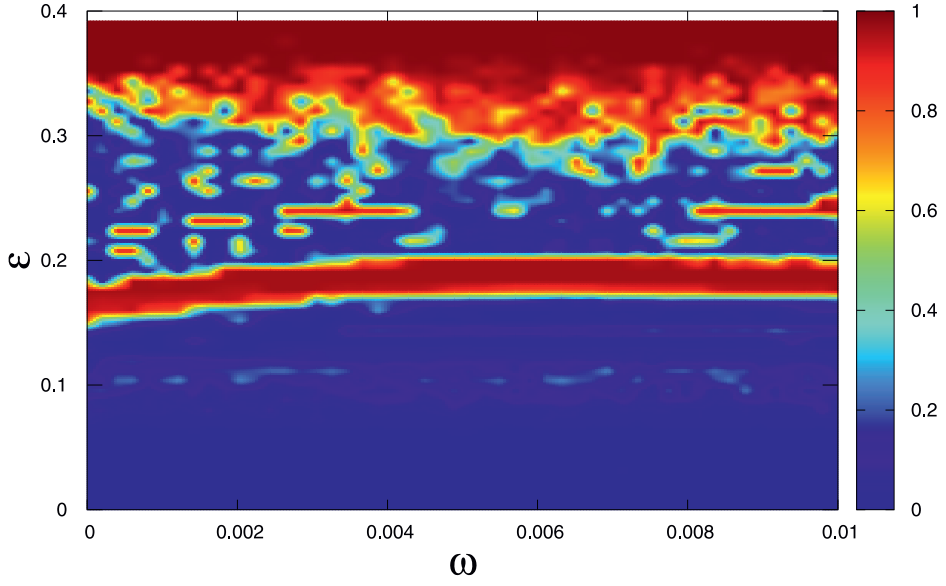

Fig. 7. Degree of coherence (in colorscale) as a function of the coupling strength ε and smoothness parameter ω, for a smoothed finite range coupling with normalized coupling radius $r = 0.32$ ($P = 160$).

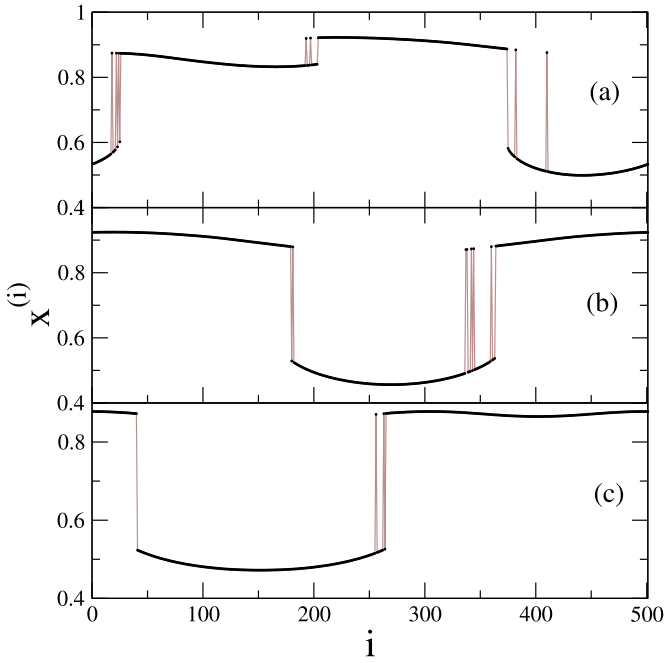

Fig. 8. Snapshots of the spatial pattern for $N = 501$ coupled chaotic logistic maps ($a = 0.38$) in the form (8), with coupling strength $\varepsilon = 0.29$, smoothness parameter $\omega = 0.006$ and coupling radius (a) $P = 30$, (b) 60, and (c) 120.

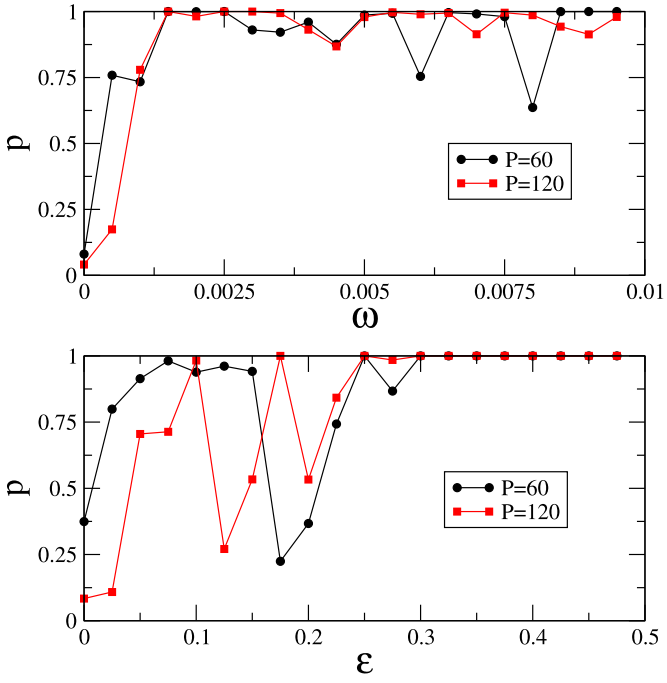

Fig. 9. (a) Degree of coherence as a function of the smoothness parameter ω, for fixed $\varepsilon = 0.18$; (b) as a function of the coupling strength ε for fixed $\omega = 0.004$. In both cases we considered a smoothed finite range coupling with two different coupling radius, namely $P = 60$ and 120.

6. Conclusions

In this work we present a generalized formulation of coupled map lattices, where the coupling among maps is non-local, for it considers not only the nearest neighbors but virtually all the lattice sites as well. The coupling strength, in this case, was supposed to depend on the lattice distance through a range function which may take on different forms, bringing about some known prescriptions like global, finite-range, power-law and exponential decay. In particular, we introduce a new non-local coupling prescription, which is a smoothed version of the finite-range type.

Analytical results were given for the Lyapunov spectrum of coupled Bernoulli (piecewise-linear chaotic) maps in terms of the range function, with application to the specific case of the smoothed finite-range prescription. The knowledge of the Lyapunov spectrum is also useful to discuss the transversal stability of the completely synchronized state of coupled chaotic maps. The synchronization manifold is transversely unstable if the second largest Lyapunov exponent is greater than zero. The analytical results we obtained for the completely synchronized state of a chaotic logistic (Ulam) map are in agreement with numerical estimates using a complex order parameter.

In the sequence we consider snapshots of spatial patterns generated by coupled map lattices with a smoothed finite-range. We obtained situations in which there is a transition from a coherent (yet not completely synchronized) to a completely incoherent state as both the coupling strength or the coupling range are varied. Using a suitable numerical diagnostic, based on the local order parameter and the counting of coherent plateaus, we analyzed how the degree of coherence varies with both the coupling range and strength. In particular, transitions from coherent to incoherent were observed as those parameters were varied.

Our results open the possibility of treating in an equal foot many different types of nonlocal couplings, and even of comparing them using similar tools. This is specially important in cases where some properties are thought to depend on the kind of nonlocal range function, like the question of permanent *versus* transient chimeras. We expect future developments along this and other lines of research.

Declaration of Competing Interest

The authors declare that they have no known competing financial interests or personal relationships that could have appeared to influence the work reported in this paper.

Acknowledgment

This work has been partially supported by the Brazilian Government Agency CNPq (Bolsa de Produtividade em Pesquisa).

References

[1] Kaneko K, Tsuda I. Complex systems: chaos and beyond: a constructive approach with applications. Berlin: Springer; 2001.
[2] Lichtenberg AJ, Lieberman MA. Regular and chaotic motion. second ed. Berlin: Springer Verlag; 1997.
[3] Kaneko K. Physica D 1989;34:1.
[4] Kaneko K. Chaos 1992;2:279.
[5] Mitchel M. Complexity: a guided tour. Oxford: Oxford University Press; 2009.
[6] Acebrón JA, Bonilla LL, Vicente CJP, Ritort F, Spigler R. Rev Mod Phys 2005;77:137.
[7] Kaneko K. Physica D 1990;41:137.
[8] Oushi NB, Kaneko K. Chaos 2000;10:359.
[9] Kuramoto Y. Prog Theor Phys 1995;94:321.
[10] Kuramoto Y, Nakao H. Phys Rev Lett 1996;76:4352.
[11] Kuramoto Y, Nakao H. Physica D 1997;103:294.
[12] Viana RL, Batista AM, Batista CAS, de Pontes JCA, Silva FAS, Lopes SR. Commun Nonlinear Sci Numer Simul 2012;17:2924.
[13] Silva FAS, Lopes SR, Viana RL. Commun Nonlinear Sci Numer Simul 2016;35:37–52.
[14] Viana RL, Batista AM, Batista CAS, Iarosz KC. Nonlinear Dyn 2017;87:1589.
[15] Liu C, Reppert SM. Neuron 2000;25:123.
[16] Gonze D, Bernard S, Waltermann C, Kramer A, Herzel H. Biophys J 2005;89:120.
[17] Aton SJ, Herzog ED. Neuron 2005;48:531.
[18] To TL, Henson MA, Herzog ED, Doyle FJ III. Biophys J. 2007;92:3792.
[19] Freeman GM Jr, Webb AB, Sungwen AN, Herzog ED. Sleep Biol Rhythms 2008;6:67.
[20] Kunz H, Achermann PJ. J Theor Biol 2003;224:63.
[21] Ueda HR, Hirose K, Iimo MJ. J Theor Biol 2002;216:501.
[22] Yamaguchi S. Science 2003;302:1408.

[23] de Haro L, Panda S. J Biol Rhythms 2006;21:507.
[24] Rogers JL, Wille LT. Phys Rev E 1996;54:R1082.
[25] Wolfrum M, Omel'chenko OE, Yanchuk S, Maistrenko YL. Chaos 2011;21:013112.
[26] Omel'chenko I, Maistrenko Y, Hövel P, Schöll E. Phys Rev Lett 2011;106:234102.
[27] Omel'chenko I, Omel'chenko OE, Hövel P, Schöll E. Phys Rev Lett 2013;110:224101.
[28] Abrams DM, Strogatz SH. Int J Bifurcat Chaos 2006;16:21.
[29] Xie J, Knobloch E, Kao HC. Phys Rev E 2014;90:022919.
[30] Omel'chenko OE. Nonlinearity 2018;31:R121.
[31] Grosu I, Banerjee R, Roy PK, Dana SK. Phys Rev 2009;80:016212.
[32] Ghosh D, Grosu I, Dana SK. Chaos 2012;22:033111.
[33] Anteneodo C, de S Pinto SE, Batista AM, Viana RL. Phys Rev E 2003;68(R):045202. Erratum: Phys. Rev. E **69**, 045202(E) (2004)
[34] Anteneodo C, Batista AM, Viana RL. Phys Lett A 2004;326:227.
[35] Viana RL, Grebogi C, de S Pinto SE, Lopes SR, Batista AM, Kurths J. Physica D 2005;206:94.
[36] Batista CAS, Viana RL. Physica A 2019;526:120869.
[37] Batista AM, de S Pinto SE, Viana RL, Lopes SR. Phys Rev E 2002;65:056209.
[38] de S Pinto SE, Lopes SR, Viana RL. Physica A 2002;303:339.
[39] Viana RL, Grebogi C, de S Pinto SE, Lopes SR, Batista AM, Kurths J. Phys Rev E 2003;68:067204.
[40] Vasconcelos DB, Viana RL, Lopes SR, Batista AM, de S Pinto SE. Physica A 2004;343(201).
[41] de Pontes JCA, Batista AM, Viana RL, Lopes SR. Physica A 2006;368:387.
[42] de Pontes JCA, Viana RL, Lopes SR, Batista CAS, Batista AM. Physica A 2008;387:4417.
[43] Kuramoto Y. Lecture notes in physics. In: Araki H, editor. International symposium on mathematical problems in theoretical physics, vol. 39. New York: Springer-Verlag; 1975. p. 420.
[44] Kuramoto Y. Chemical oscillations, waves, and turbulence. New York: Springer-Verlag; 1984.
[45] Sethia GC, Sen A. Phys Rev Lett 2014;112:144101.